

Vis-A-Ware: Integrating Spatial and Non-Spatial Visualization for Visibility-Aware Urban Planning

Thomas Ortner, Johannes Sorger, Harald Steinlechner, Gerd Hesina, Harald Piringer, and Eduard Gröller

Abstract—3D visibility analysis plays a key role in urban planning for assessing the visual impact of proposed buildings on the cityscape. A call for proposals typically yields around 30 candidate buildings that need to be evaluated with respect to selected viewpoints. Current visibility analysis methods are very time-consuming and limited to a small number of viewpoints. Further, analysts neither have measures to evaluate candidates quantitatively, nor to compare them efficiently. The primary contribution of this work is the design study of Vis-A-Ware, a visualization system to qualitatively and quantitatively evaluate, rank, and compare visibility data of candidate buildings with respect to a large number of viewpoints. Vis-A-Ware features a 3D spatial view of an urban scene and non-spatial views of data derived from visibility evaluations, which are tightly integrated by linked interaction. To enable a quantitative evaluation we developed four metrics in accordance with experts from urban planning. We illustrate the applicability of Vis-A-Ware on the basis of a use case scenario and present results from informal feedback sessions with domain experts from urban planning and development. This feedback suggests that Vis-A-Ware is a valuable tool for visibility analysis allowing analysts to answer complex questions more efficiently and objectively.

Index Terms—Geographic/geospatial visualization, visual analytics, integrating spatial and non-spatial data visualization, focus + context techniques, coordinated and multiple views

1 INTRODUCTION

THE designation of urban areas for construction is typically followed by an open call, where architecture firms submit building designs. In case of a redesignation of inner city areas, it is common that such a call yields up to 30 candidate buildings. A new building in such an area possibly affects the cityscape, and typically sparks controversy between various stakeholders, such as neighbors, the property developer, and decision-makers from politics and urban development.

Although there are many factors to consider when comparing candidates, visibility analysis plays an increasingly important role especially in controversial cases, for instance, if the occlusion of a landmark is involved. Typically, experts from urban surveying conduct the following series of analyses to support an informed discussion between decision-makers: creating visibility and landmark occlusion maps for each candidate, photo montages overlaying real images with virtual candidate buildings, and offline renderings for each building from a few viewpoints. Further, haptic models of each candidate and of the surroundings are created to explore different scenarios during a jury discussion.

- T. Ortner, J. Sorger, H. Steinlechner, G. Hesina, and H. Piringer are with the VRVis Research Center, Vienna 1220, Austria. E-mail: {ortner, sorger, steinlechner, hesina, piringer}@vrvis.at.
- E. Gröller is with the TU Wien, Vienna 1040, Austria. E-mail: groeller@cg.tuwien.ac.at.

Manuscript received 30 June 2015; revised 6 Dec. 2015; accepted 16 Jan. 2016. Date of publication 22 Jan. 2016; date of current version 4 Jan. 2017.

Recommended for acceptance by G. Andrienko.

For information on obtaining reprints of this article, please send e-mail to: reprints@ieee.org, and reference the Digital Object Identifier below.

Digital Object Identifier no. 10.1109/TVCG.2016.2520920

1.1 Task Analysis

Cooperating with experts from urban surveying, urban planning, and urban development we identified the following tasks in the context of 3D visibility analysis:

- Line-of-sight (LoS) and landmark occlusion analysis.
- Selection of relevant viewpoints for renderings and montages.
- Analysis of the visual impact on the cityscape.
- Comparison of candidates with respect to visual impact.

1.2 Current Challenges

In the current visibility analysis process, the impact of candidates on the cityscape is mostly judged by aesthetics and visual appeal, based on montages, renderings, and the haptic model. Apart from a potential subjective bias, a pure qualitative assessment restricts the analysis process to a small number of viewpoints.

For a quantitative analysis, geographic information systems (GIS) are used. For example, in landmark occlusion analysis, a mask is computed which indicates areas in a city from where a landmark is visible. Computing 2D visibility maps for up to 30 candidates is very time-consuming and GIS tools do not offer functionality to compare dozens of map layers efficiently. Furthermore it is cumbersome to extend the described method to a more granular quantification of visibility beyond ‘landmark is visible’ and ‘landmark is occluded’.

1.3 Design Goals

Based on previous observations, we derived the following design goals, for a tool supporting the aforementioned tasks:

- **G1:** Compute intuitive metrics for quantifying the visual impact of candidates with respect to specific viewpoints.
- **G2:** Tight integration of spatial views and non-spatial views to allow for a linked analysis of quantitative and qualitative data.
- **G3:** Fast identification of candidates or viewpoints exhibiting high visual impact values.
- **G4:** Providing an overview of the spatial distribution of viewpoints with high visual impact.
- **G5:** Intuitive filtering, ranking, and comparison of candidates as well as viewpoints.
- **G6:** Incorporating exploration and visualization metaphors users are already familiar with from existing tools.

1.4 Contributions

The primary contribution of this paper is the design study of Vis-A-Ware, a tool tailored to the 3D visibility analysis of building alternatives in urban environments. We illustrate the applicability of Vis-A-Ware based on an artificial use case scenario and present feedback by experts from urban planning, urban development, and urban surveying. As a secondary contribution we present the quantification of visual impact by combining multiple metrics derived from the urban planning literature [1].

2 RELATED WORK

2.1 Visibility Analysis

Determining the visibility of 3D objects is an essential and well-researched topic in the field of real-time rendering. The most important application is occlusion culling in order to avoid drawing invisible objects. This reduces potential overdraw in complex 3D scenes [2]. As presented by Bittner et al. [3], most occlusion culling implementations spatially subdivide the 3D scene. Brunnhuber et al. [4] present a system to evaluate signage for pedestrians inside large buildings. They use projections, similar to shadow mapping, originating from simulated pedestrians to determine how good signs are potentially perceivable by a person. Although they use a fine-grained concept of visibility, their tool does not offer any analysis capabilities beyond false-color mapping. Visibility analyses are a standard feature in many geographic information system applications, such as ArcGIS [5]. Typical tools include line-of-sight intersections for urban scenes, or viewshed analysis in rural areas. These computations are often time-consuming and are therefore performed offline, while results are encoded into map layers. Geoweb3D [6] alleviates this rigidity and offers interactive viewshed evaluations in a GIS environment by using a technique similar to Brunnhuber et al. [4]. None of these tools allow experts the comparison of multiple viewpoints, or to determine visibility values for individual buildings. Doraiswamy et al. [7] developed several metrics to quantify the quality of floor views in order to create efficient building designs in terms of effort and real-estate value. Their system focuses on the optimization of design parameters to support the iterative design process between architects and developer clients.

2.2 Decision-Making & Ranking

Multiple-Criteria Decision Analysis (MCDA) refers to making a decision in the presence of multiple, usually conflicting criteria. Many authors deal with MCDA in the context of multi-objective optimizations [8], [9]. The described methods are typically applied to multiple-criteria design problems such as in visual parameter-space exploration, where a large or infinite number of design alternatives is present [10], [11], [12].

In contrast, multiple-criteria evaluation problems contain a finite number of alternatives, which is often the case in geo-spatial analyses, such as automatic MCDA analysis in the context of land-suitability analysis [13]. Andrienko and Andrienko [14] extend a GIS application by non-spatial views in order to gain insight into automatic MCDA algorithms. Bruckner and Möller [15] cluster visual results from an infinite design space into distinct finite alternatives. Sorger et al. [16] use a weighted ranking view to evaluate lighting setups for MCDA in the context of lighting design. Gratzl et al. [17] present a tool called *LineUp* to intuitively rank a large number of alternatives. While *LineUp* focuses on tackling ranking problems in general by weighted scores, our work concentrates on ranking and efficiently exploring distributions in an urban planning use case. Our ranking approach and design choices were inspired by their work.

Several authors present tools to support decision-making in the context of urban planning and urban development. Andrienko et al. [18] present a framework to aggregate and analyze large sets of spatio-temporal data regarding traffic and crime analysis. Zhang et al. [19] present a framework for detecting, aggregating, and analyzing public utility service problems through coordinated multiple views (CMVs). Zeng et al. [20] quantified mobility and developed a novel visualization letting users explore and compare branches in a public transportation system. They do not address visibility problems in a 3D space as we do. Ferreira et al. [21] aim to provide an application that gives a holistic overview of urban data, including visibility calculations. Compared to our approach, their work does not offer a way to efficiently compare multiple building candidates. It also does not consider the special requirements that urban planners have to take into account when approving a new building, as for instance, multiple lines of sight and signature viewpoints.

2.3 Integrating Spatial and Non-Spatial Visualizations

CMV in combination with linking and brushing present a valuable tool to explore different aspects of data in different views. In the context of CMV many authors integrated non-spatial visualizations in order to gain insight into complex spatial data, as for instance, in the areas of computational fluid dynamics [22], medical visualization [23], [24], or neurobiology [25]. Chang et al. [26] integrate a spatial view with non-spatial visualization views to explore spatial patterns in demographic data. Butkiewicz et al. [27] extend the work of Chang et al. [26] by a spatial probe metaphor to explore clusters, which is then applied to various GIS-like applications. Ribicic et al. [10] use visual analytics in order to evaluate barrier configurations in simulated flooding scenarios.

3 PROBLEM ABSTRACTION

3.1 Problem Space

If a municipal area is designated for a construction project, it is statutory for the local government to initiate a call for proposals. Multiple architecture offices submit their proposed buildings, which we will refer to as *candidates*. For prestigious projects such a call can yield up to 30 candidates. These candidates are then checked against hard criteria, such as maximum height, minimum energy efficiency, minimum floor space, or office to apartment ratio. Since these criteria are known by the architecture offices beforehand only a small number of candidates is discarded in this process. Besides meeting these hard constraints, a candidate is required to ‘visually fit’ into the cityscape.

For this purpose, urban planning experts produce a visibility analysis, often consisting of *line-of-sight* analyses, rendered still images from certain *viewpoints* in the city, and photomontages overlaying real images with candidate renderings. LoSs are point to point connections from vantage points to typically a *landmark*, for instance, the LoS from a hill top to a cathedral. If a candidate severely occludes a landmark, it is likely to be rejected. Additionally, urban planning experts select a handful of relevant viewpoints. Such viewpoints are chosen through experience and are then used for rendering still images and creating photomontages. The resulting images support a qualitative evaluation in a jury discussion.

So far candidates violating hard criteria were already discarded, but other non-visibility parameters of the remaining candidates still factor into a final decision. In this regard, the partitioning of floor space into offices, apartments, shops, or hotel rooms is relevant since potential revenues can be derived from that. However, we consider these parameters as out-of-scope of Vis-A-Ware for two reasons: First, our collaborators are only concerned with the visibility analysis of candidates and could not provide this data. Second, algorithms and tools for MCDA of parameters not concerning 3D visibility are already widely in use [13], [14].

Factors that are not directly related to the building design itself are outside of the problem space as well, since the site for development is already chosen. Examples are the connection to public transport [20], the access to public infrastructure (e.g., shops, schools, museums, etc.), or the proximity to recreational areas [21].

3.2 Quantifying Visual Impact

A qualitative analysis of n candidates with respect to m viewpoints involves $n * m$ comparisons. To support this process with visual analytics methods, we need to quantify the visual impact that candidates cause on specific viewpoints. Urban planning researchers have sought to quantify the visual impact based on the idea that geometric properties relate to the perception of urban space [1]. Following *Viewsphere*, introduced by Yang et al. [1], we derived four visual impact metrics (VIMs): *landmark occlusion*, *candidate visibility*, *openness occlusion*, and *sky occlusion*. We discussed the VIMs with urban planning experts, who confirmed that these metrics are well-suited for quantifying the visual impact. The described metrics are derived from false color images, as illustrated in Fig. 2c. Their computation will be described in Section 5. VIMs are defined as follows:

- *Landmark occlusion*: Image area of landmarks occluded by a candidate.
- *Candidate visibility*: Image area covered by a candidate. Describes how prominent a candidate is from a specific viewpoint.
- *Openness occlusion*: Image area of open space (with respect to existing buildings and terrain) covered by a candidate. Openness is based on the Spatial Openness Index presented by Yang et al. [1].
- *Sky occlusion*: Image area of the sky covered by a candidate.

4 SYSTEM OVERVIEW

After abstracting the problem space we are confronted with a multiple-criteria decision problem where users compare and evaluate a finite set of solutions. Due to the mixture of qualitative (aesthetic appeal and perception) and quantitative aspects (VIM values) in this scenario, there is typically no single optimal candidate. The goal of Vis-A-Ware is to support urban planners in reducing the set of candidates and viewpoints effectively and efficiently without relying on time-consuming offline renderings or GIS analyses. The resulting reduced set is then presented to decision-makers as a foundation for an informed jury discussion.

We tackle this problem in several steps which will be outlined in the subsequent sections. From the problem space abstraction we derived a flexible data model which represents candidates, viewpoints, and VIMs (Section 5.1). We developed an image-based approach to quantify visibility and quickly evaluate candidates in hundreds of viewpoints (Section 5.2). We process the resulting VIM data by normalization and binning to make it more intuitive and comparable (Section 5.3). We provide a novel ranking view (Section 7.1) to explore the processed VIM data through means of ranking, focus and context, and detail-on-demand. The ranking view is linked with a 3D view (Section 7.2) for assessment of spatial distribution and an image viewer (Section 7.3) for qualitative comparison.

5 VISUAL IMPACT METRIC COMPUTATION

5.1 Data Model

Our data model consists of the following entities: *candidate*, *viewpoint*, and *VIM*. The combination of a viewpoint, a candidate, and a set of VIMs we denote as an *evaluation*. Each evaluation is associated with a rendered image of the scene. The entire evaluation data can be organized in an $n * m$ matrix, where n and m are the numbers of candidates and viewpoints, respectively (see Fig. 3a). In our case, each cell of this matrix contains a vector of four VIM values for landmark occlusion, candidate visibility, openness occlusion, and sky occlusion.

From this data layout we derive two lookup tables as shown in Fig. 3b. The table on the left shows candidate scores for each viewpoint (viewpoint-major) while the table on the right shows impacted viewpoints for each candidate (candidate-major). We denote the entity by which a row of the lookup-table is identified as *major*, whereas the entities that form the content of each row are denoted as *minor*. Switching, from a viewpoint-major to a candidate-major representation or vice-versa, will be referred to as *transposing*.

For our approach of a quantitative visibility analysis, we interpret viewpoints and LoSs as measurement probes for the visibility in the 3D scene. We define each viewpoint by its spatial position, orientation, and horizontal field of view (FOV). We model a LoS as a special case of a viewpoint with a narrow FOV. The cityscape, where the visibility analysis is performed, is represented through a 3D city model and a digital elevation model of the terrain.

5.2 Image-Based Approach

For evaluating the visual impact that candidates cause on a viewpoint, we render the view from the respective viewpoint in false colors, as illustrated in Fig. 2. We turned off lighting and shading and defined unique colors for each of the following components of the scene: landmarks (red), existing buildings (purple), terrain (green), sky (blue), and candidate buildings (orange). We render a single false-color image for each candidate (Fig. 2b). We further render an image containing the *existing situation* without any candidate building (Fig. 2a). This lets us compute the difference of each VIM for each candidate in comparison to the existing situation. Finally, we render an image with all candidates at once (Fig. 2d), which we use for normalization, as it will be described in the next section. After each rendering, the number of pixels belonging to each unique color is counted. As a result, we get the area each component covers in the rendering from the current viewpoint. In addition to the false-color renderings, we save a rendered image of the current viewpoint and candidate combination for the qualitative analysis. The presented approach is straightforward to implement, fast, and offers a pixel-accurate visibility-evaluation method. The current implementation summarizes all landmarks into a single score. Our approach is also compatible with handling multiple distinct landmark scores. This would require an additional VIM per landmark in the data table and an additional color in the false-color rendering.

5.3 Normalization and Binning

Our image-based evaluation approach yields numbers of pixels. Pixel counts as raw output values are unintuitive and since different parts of the scene naturally cover vastly different areas (e.g., sky versus existing buildings) it is difficult to compare candidates or viewpoints across metrics. Therefore we decided to normalize our VIM data. This is straightforward for the landmark occlusion metric (LM):

$$\hat{LM}_i = (LM_0 - LM_i)/LM_0. \quad (1)$$

\hat{LM}_i is the ratio of the landmark area occluded by a candidate i ($i = 1 \dots n$). It is described by the difference of landmark pixels of the existing situation (LM_0) and landmark pixels in the image containing candidate i (LM_i) divided by LM_0 .

Our users confirmed that it is intuitive to measure landmark occlusion in percentage of landmark area occluded by a candidate. However, we cannot normalize openness occlusion and sky occlusion in the same way, since they only yield very small relative differences which are difficult to interpret. Both are also very sensitive to the viewpoint orientation, for instance, when tilting the viewpoint slightly

upwards the number of sky pixels increases substantially, while the number of existing-building- and terrain-pixels decreases. Since there is no candidate building in the existing situation, we tried to measure the visibility of a candidate relative to the total number of image pixels, which as well did not yield intuitive results. To address this we compute the normalized VIM value \hat{Vim}_i for candidate i in a given viewpoint as follows:

$$\hat{Vim}_i = (Vim_0 - Vim_i)/(Vim_0 - Vim_a), \quad (2)$$

where Vim_0 is the number of pixels of a VIM in the existing situation, Vim_i is the number of pixels in the ‘single candidate’ image containing candidate i , and Vim_a is the number of pixels in the ‘all candidates’ image as illustrated in Fig. 2d.

In case of the candidate visibility metric the value of Vim_0 equals 0. This is due to the fact that there is no candidate building in the existing situation. For computing the openness occlusion metric, we add the pixel counts of the existing buildings and the terrain in the respective images.

After normalization, the VIM values are scaled to percentages and are binned into four classes: $[0 - 25[$, $[25 - 50[$, $[50 - 75[$ and $[75 - 100]$, which we denote as *low*, *medium*, *high*, and *very high*, respectively. This makes the individual scores more intuitive than actual percentages. The higher the values are, typically the more negative is the visual impact. However, in a use case where urban planners want to create a new landmark building they would want to choose a candidate with a high or very high candidate visibility. We additionally use the ‘all candidates’ image to compute a ratio describing the relevance of a viewpoint. For this we divide the number of pixels covered by all candidates by the total number of image pixels. This value indicates how much of the candidate geometry is actually visible from this viewpoint and implies how important visual-impact values in this viewpoint are. Since these percentages are even more difficult to interpret we bin them into three classes as depicted in Fig. 2e: $[0 - 5]$, $[5 - 10]$, and $[10 - 100]$, corresponding to *small*, *medium*, and *large* coverage. We designed this classification empirically, based on feedback from our experts.

6 USE CASE SCENARIO

We introduce a use case scenario, in order to make the discussion of design decisions in Section 7 and the subsequent demonstration of the applicability of Vis-A-Ware in Section 8 more tangible.

In cooperation with the Vienna department of urban surveying we obtained a detailed 3D city model of Vienna and of the underlying terrain. Since the rights for each submitted candidate building lie with the respective architecture firm, it was not possible to use data from a real call for proposals, therefore this is an artificial use case. As illustrated in Fig. 4a, we created 20 candidate buildings of various shapes and sizes in accordance with our experts and placed them in a project area near Vienna’s north railway station (Fig. 4b). Each candidate is identified by a letter from A to T. In the traditional workflow expensive computations limit

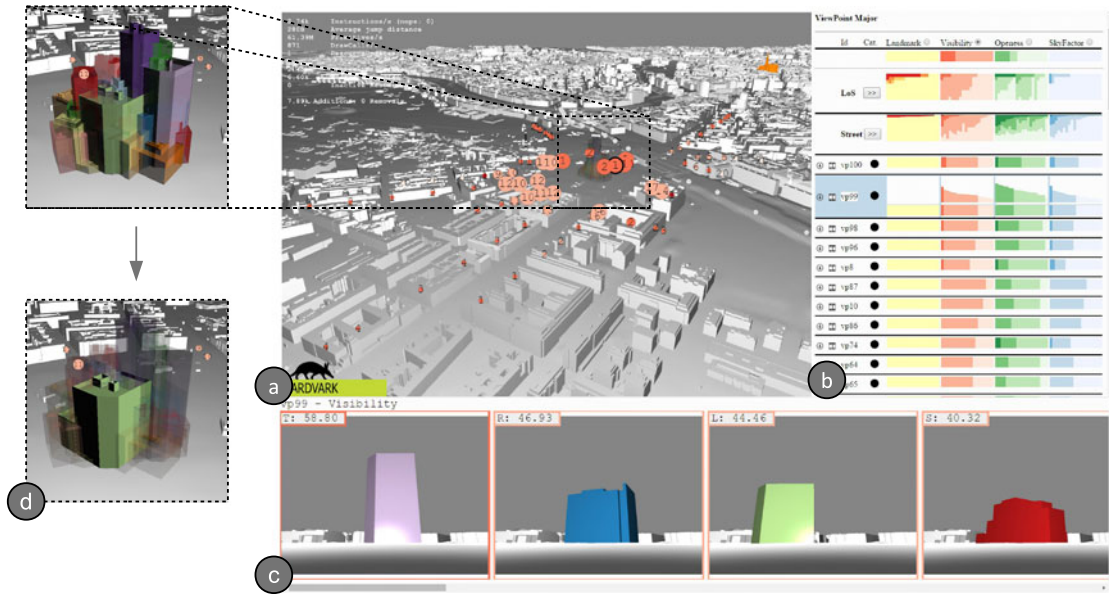


Fig. 1. An overview of Vis-A-Ware, a tool supporting 3D visibility analysis in urban planning. It features the following coordinated views: (a) a 3D spatial view to investigate spatial relations between planned structures and viewpoints, (b) the transposable ranking view to analyze derived visibility metrics, and the filmstrip (c) filmstrip for a qualitative comparison of single-building renderings. (d) 3D representations of the candidate buildings are blended together, hovering in linked views renders the respective candidate as solid.

the analysis to a handful of viewpoints. However, domain experts stated that using more viewpoints would be desirable, for instance, along certain streets or railroad tracks. Since this restriction does not apply to Vis-A-Ware, we placed 53 viewpoints in the vicinity of the planning area divided into three categories: ‘LoS’ (7), ‘Street’ (32), and ‘Train’ (14). The scene further includes one landmark, the St. Stephen’s Cathedral colored in orange as shown in the background of Fig. 4b.

7 VISUALIZATION AND INTERACTION DESIGN

Vis-A-Ware consists of three coordinated views: The *transposable ranking view* (TRV) (Fig. 1b) is the center piece of Vis-A-Ware and allows users to interactively explore all quantitative evaluation data. The *3D spatial view* (Fig. 1a) offers an interactive exploration of the cityscape, candidates, and viewpoints. Finally, the *filmstrip* (Fig. 1c) provides a side-by-side comparison of candidate renderings from specific viewpoints for a qualitative evaluation.

7.1 Transposable Ranking View

The TRV was designed with the following goals in mind:

- **Overview** of visual impact results of candidates and viewpoints. (G4)
- Intuitive **filtering** of candidates and viewpoints. (G5)
- **Detail-on-demand** showing individual visual impact values. (G1)
- **Ranking** of candidates or viewpoints by individual VIMs. (G3, G5)
- **Comparison** of candidates by multiple VIMs. (G2, G5)

The TRV is a tabular view, where the rows either represent candidates or viewpoints (compare to lookup table in Fig. 3), while the individual VIMs determine the columns of this table. Each cell contains the distribution of minor

entities regarding a specific VIM. For instance, Fig. 5 shows VIM values of candidates for each viewpoint, since the TRV is in viewpoint-major mode. Indicated by the bar charts, the three cells shown in Fig. 5b contain candidate visibility, openness occlusion, and sky occlusion values for each candidate.

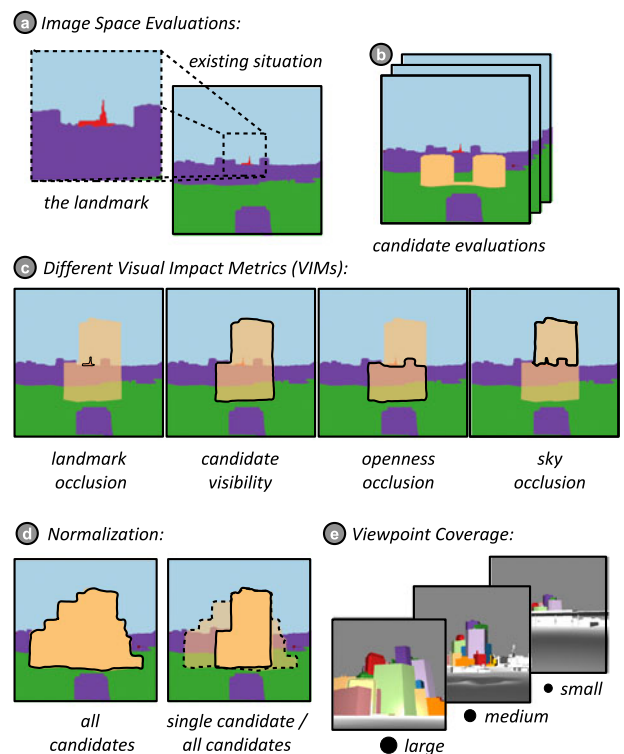


Fig. 2. False color image evaluation, (a) of existing situation, (b) for each candidate. (c) Four metrics to quantify visual impact: landmark occlusion, visibility, openness, sky occlusion. (d) ‘All candidates’ evaluation for normalization of metrics (except for the landmark occlusion metric) (e) Ratio of ‘all candidates’ to image size: large, medium, small.

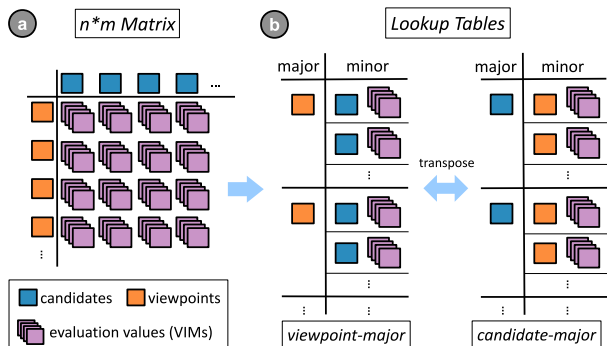


Fig. 3. Data Model: (a) Evaluations are represented by an $n*m$ matrix of candidates and viewpoints. Each combination holds a series of VIM values. (b) This representation is transformed into a lookup table either governed by viewpoints (viewpoint-major) or by candidates (candidate-major).

7.1.1 Visual Encoding

The TRV in Fig. 5 depicts the evaluation data in viewpoint-major mode showing one row for each viewpoint. The *detail bar charts* in Fig. 5a show the VIM scores of each candidate in a single viewpoint. The detail bars are sorted by candidate score (i.e., bar height) and encode the respective class into the color of a bar. Through the color coding and the sorting we can condense the bar charts to *stacked bar charts* as depicted in Fig. 5b, which allows us to efficiently display a large number of rows. If hovering over a row it expands and reveals the detail bar charts providing detail-on-demand. Hovering over individual detail bars opens a tooltip which shows the exact VIM value of a candidate (Fig. 5c). This detail hovering further triggers a peek-brush [28] interaction which shows the occurrence of the respective candidate in all other VIM distributions by showing the candidate's letter in the stacked bar chart. As illustrated in Fig. 5b the rank of a candidate within a distribution is preserved which effectively conveys the ranks of a candidate for each VIM and each viewpoint.

We used colorbrewer [29] to pick color schemes for the visual encoding of the classes of the different VIMs. For candidate visibility, openness occlusion, and sky occlusion, we chose sequential four-class single hue color schemes, with the respective hues red, green, and blue. Since the landmark evaluation is a more decisive VIM and slightly differs in computation from the others we chose a multi-hue color scheme from

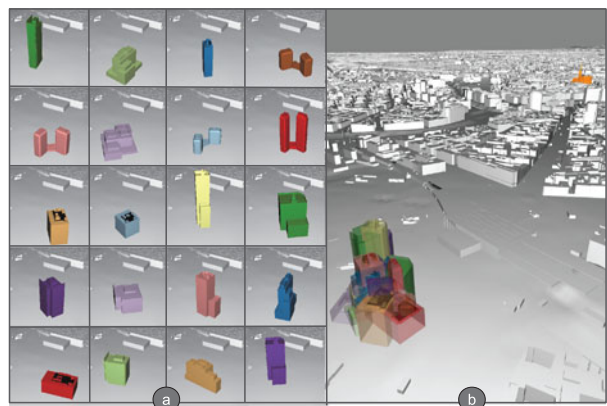


Fig. 4. (a) 20 individual candidate buildings of different size and shape. (b) Planning area near railway station and a landmark cathedral (orange) in the back.

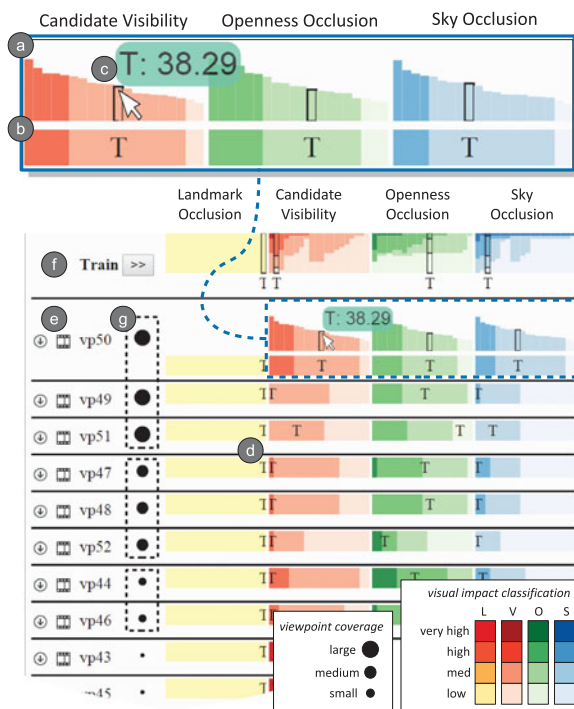


Fig. 5. Transposable Ranking View: (a) Detail bar charts showing individual VIM values of each candidate. (b) Stacked bar charts as a compact version of VIM distributions. (c) Linked peek-brushing shows detail-on-demand tooltip and a candidate's position within all other VIM distributions. (d) Rows are ranked by distribution scores of the selected VIM - in this case candidate visibility. (e) The arrow-icon loads the perspective of a viewpoint into the 3D view, while the film-icon loads respective screenshot data into the filmstrip. (f) Each category of viewpoints is collapsible and features a heatmap-like aggregation of VIM scores. (g) Viewpoints are grouped by their coverage value, which is indicated by the size of the black circles.

yellow to red. The color coding can be adapted and easily replaced with other colorbrewer schemes.

7.1.2 Focus, Filter, and Transpose

The workflow supported by the TRV is a sequence of focus, filter, and transpose interactions which allow users to investigate evaluations with respect to candidates and viewpoints. When clicking on individual stacked bars (Fig. 6a) the respective minor entities are added to the focus set while the others are considered as context. To visually distinguish focus and context we create *split stacked bars*. As illustrated in Fig. 6b the focus on the left is rendered at full height, while the stacked bars of the context on the right are rendered at reduced height. This partition of minor entities into focus and context is reflected in all stacked bar charts. An arbitrary concatenation of focus interactions allows the creation of a focus set by selecting any number of stacked bars (Fig. 6c). Through keyboard interaction the minor entities of the context set are filtered from the TRV (Fig. 6d). The transpose interaction allows users to shift the focus of the analysis from viewpoints to candidates or vice versa by switching between candidate-major and viewpoint-major mode. For instance, Fig. 6d shows viewpoints as rows (viewpoint-major), while after transposing Fig. 6e shows candidates as rows (candidate-major).

For demonstration purposes Fig. 6 illustrates the identification of candidates which are most prominent as seen from

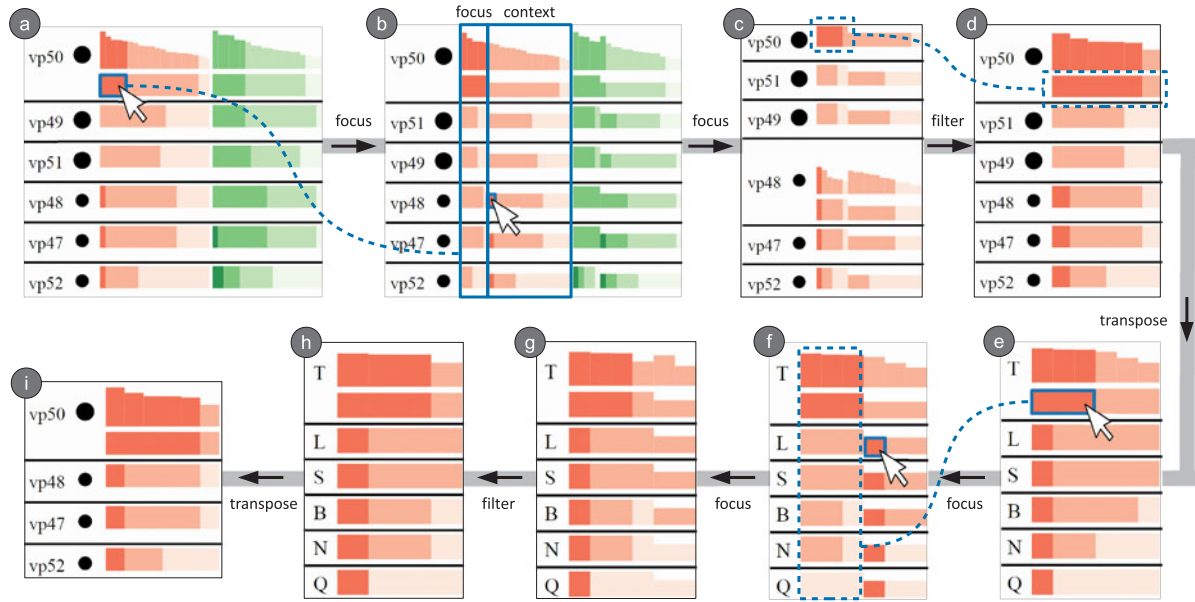


Fig. 6. Focus, Filter, and Transpose workflow for reducing candidate and viewpoint sets: (a) 20 candidates impact six viewpoints, selection of high class visibility candidates in vp50 (b) higher bars encode selected candidates (in focus). Selection of additional high class visibility candidates in vp48. (c) The focus set covers all candidates exhibiting high visibility values. (d) Candidates are filtered to the focus set, dropping all candidates which do not exhibit high visibility values in any viewpoint. (e) Transposed view: candidates are now rows, the selection now affects viewpoints highly impacted by candidate T. (f) Selection is extended by other highly impacted viewpoints. (g) All highly impacted viewpoints are now part of the focus set. (h) Set is filtered to the focus set. (i) Transpose to see the set reduced to six candidates in four viewpoints.

the railway (compare Section 8.2) by depicting relevant cut-outs of the TRV for each interaction (Figs. 6a-6i). The displayed data set comprises twenty candidates and six relevant viewpoints from the ‘Train’ category. To focus on candidates users are able to select individual stacked bars. For example, selecting the high visibility scores in *vp50* in Fig. 6a splits the stacked bar charts into two charts as shown in Fig. 6b. The split stacked bars allow users to judge how the candidates in focus impact other viewpoints. Users may select additional high class bars among the context candidates (Fig. 6b), which are then added to the focus set (Fig. 6c). All high impact classes are in focus so users filter the context candidates (Fig. 6c). This expands the focus set to cover the whole width of the chart (Fig. 6d). For reducing the set of viewpoints transposing the TRV makes the candidates the major entities, while the viewpoints are encoded into the stacked bars (Fig. 6e). This enables the selection of viewpoints containing a high visibility value for candidate *T* (Fig. 6e). Fig. 6f indicates that other viewpoints exhibit high impact values from other candidates as well, which can be included into the selection. All viewpoints with high classes are in focus (Fig. 6g). Filtering of the context leaves six candidates and four viewpoints (Figs. 6h and 6i).

7.1.3 Ranking

To quickly identify highest scoring candidates or highly impacted viewpoints the rows of the TRV must be sortable by any VIM. Therefore we need to assign an unambiguous score to any distribution of visual impact. This score has to ensure that, for instance, a viewpoint exhibiting a single candidate in the very high class is always ranked higher than any viewpoint not containing a very high VIM score. Thus we use the mathematical concept of a numeral system to assign a score to each stacked bar chart:

$$score(d) = \sum_{i=1}^p x_i \cdot b^{i-1} \quad (3)$$

where d is the distribution of VIM values, p is the number of classes used in d , b is the maximum number of items in one class (total number of viewpoints or candidates) and x is the actual number of items in class i . As it can be seen in Figs. 5 and 6, viewpoints are ordered within their category depending on their candidate visibility values. In terms of a numeral system b refers to the base while p represents the number of digits.

7.1.4 Categories, Aggregation, and Grouping

Not all viewpoints in the city have the same semantic meaning, as there are LoSs, single pedestrian viewpoints, pedestrian viewpoints along a street or viewpoints along a railway section. Vis-A-Ware thus supports to divide the set of viewpoints into user-defined categories. Each category is represented by a collapsible table while each category header features an aggregation bar chart per VIM (Fig. 5f). The aggregation bar charts show a vertical stacked bar for each candidate, while each bar represents the number of viewpoints per VIM class.

This transposed aggregation allows the quick identification of candidates, which exhibit high values in a category. Further, it presents a heat-map-like overview of VIM distributions and indicates if that category is worth exploring. For the target use case of deciding between individual candidates, only viewpoints are reasonably divided into semantic groups, and therefore the collapsible categories are only present in viewpoint-major mode. Within each category viewpoints are further grouped by their coverage value (see Fig. 2e) encoded by a black circle next to the viewpoint identifier as illustrated in Fig. 5g. Three different circle

sizes represent the three different coverage classes large, medium, and small. If a viewpoint category is collapsed its viewpoints are excluded from the TRV. Consequently, if transposing to candidate-major mode, these viewpoints do not appear in the stacked bar charts.

7.1.5 Integrated Interaction

The peek-selection interaction through hovering as discussed in Section 7.1.1 allows users to quickly highlight candidates or viewpoints in all charts (Fig. 5c). The TRV in viewpoint-major mode features an arrow-icon (Fig. 5f), which if clicked changes the perspective of the 3D spatial view to match the perspective of the selected viewpoint. Clicking the film-icon loads the associated data row into the filmstrip for a qualitative evaluation (Fig. 1c). The ranking, the filtering, and the peek-selection are coordinated with the 3D spatial view and the filmstrip. How these views react to these interactions will be explained in the Sections 7.2 and 7.3, respectively.

7.2 3D Spatial View

The 3D spatial view depicts a 3D geovirtual environment, consisting of a city model, landmarks, candidate buildings, and circular glyphs representing the positions of the viewpoints. Candidates are rendered as semi-transparent colored 3D models, which enables the users to inspect multiple buildings at once. Since it is not possible to pick distinguishable colors for about 30 candidate buildings, we chose a set of 10 repeating qualitative colors [29]. The set of displayed candidates can be reduced through filtering in the TRV. Peek-brushing of candidate entities in the TRV or the filmstrip causes 3D representations of candidates in the 3D spatial view to be rendered completely opaque, as illustrated in Fig. 1d. This enables users to compare the spatial properties of one particular candidate with respect to the other candidates of the currently displayed set.

As it is depicted in Fig. 1a, we display an aggregated view of the candidate distribution in each viewpoint as a circular glyph. This glyph comprises a colored circle containing a number and is displayed at the spatial position of its respective viewpoint. This enables the assessment of the spatial distribution of VIM values across the city scene. If major entities in the TRV are ranked by a specific VIM, this VIM is encoded by the color of the circles. The specific color of the circle corresponds to the highest class in its distribution, while the number in it is the number of candidates in this respective class. The coverage value of a viewpoint is mapped to the area of the circle. This enables users to judge the extent of the visual impact, with respect to the selected VIM, across the city. Viewpoints with a small coverage are de-emphasized. Only the viewpoints of expanded categories in the TRV are shown in the described encoding. All other viewpoints are considered as context and are rendered as gray circles. Peek-brushing of viewpoints in other views causes the highlighting of the respective circles in the 3D spatial view by emphasizing their border line.

7.3 Filmstrip

The domain experts are accustomed to side-by-side comparisons for a qualitative analysis of candidates. We chose a

filmstrip metaphor, similar to Bruckner and Möller [15], to display the images which are associated with each evaluation in a side-by-side layout as depicted in Fig. 1c. Clicking onto the film-icon in the TRV loads the content of the respective row into the filmstrip. Depending on the current mode of the TRV, the filmstrip either shows the images of all candidates in one viewpoint (viewpoint-major) or one candidate in all viewpoints (candidate-major). A header line shows the identifier of the major entity, i.e., the row, while a rectangle in the upper left corner of each image displays the name and VIM value of each minor entity.

An image's border color encodes the impact class of the corresponding candidate-viewpoint pair. The displayed VIM corresponds to the VIM currently selected for ranking in the TRV. The images displayed in the filmstrip are filtered depending on the filter criteria specified in the TRV. Hovering over images causes highlighting of the respective entities in the other views.

8 VISIBILITY ANALYSIS

In collaboration with domain experts from urban planning we formulated three exemplary questions based on the traditional qualitative visibility-analysis workflow. We demonstrate how the developed views and metrics support the users to navigate through evaluation results and inspect selected subsets of candidates and viewpoints qualitatively.

8.1 Which Candidates Cover a Landmark and How Strong is the Occlusion? (Q1)

Severely occluding a landmark along a LoS is an exclusion criterion for candidates. To focus on LoSs users collapse all categories except the 'LoS' one. The remaining viewpoints are ranked by the landmark occlusion metric as shown Fig. 7a. Hovering over the aggregation view reveals that F and T cause very high landmark occlusions (Fig. 7a). Apparently only the LoSs $vp5$ and $vp4$ are affected, which is indicated by the absence of orange bars in $vp6$ and $vp3$. To focus on very high and high classes of landmark occlusion, users are able to select the respectively colored bins in $vp4$. The split stacked bars in Fig. 7b show that other candidates than the ones previously selected cause very high and high occlusions in $vp5$. Users select the respective candidates in $vp5$ and filter the TRV to the selected set of candidates (Fig. 7c). Inspection of the detail bar charts uncovers, for instance, that F has a very high score in $vp4$ but only medium impact in $vp5$ (Fig. 7d). To analyze the individual impact values of the selected candidates with respect to $vp4$ and $vp5$ analysts transpose the TRV (candidate-major) (Fig. 7e) and focus and filter so that only viewpoints $vp4$ and $vp5$ remain (Fig. 7f). The data set is now reduced to five candidates in two viewpoints. Analysts can now evaluate each candidate qualitatively by opening the filmstrip, depicting the selected candidate as seen from two viewpoints. As Fig. 7g shows, the landmark occlusions of F in $vp4$ and T in $vp5$ are indeed very high.

8.2 Which Candidates Are Most Prominent as Seen from the Railway? (Q2)

High visibility is not necessarily a negative aspect of a candidate. Often city administrations want to construct a

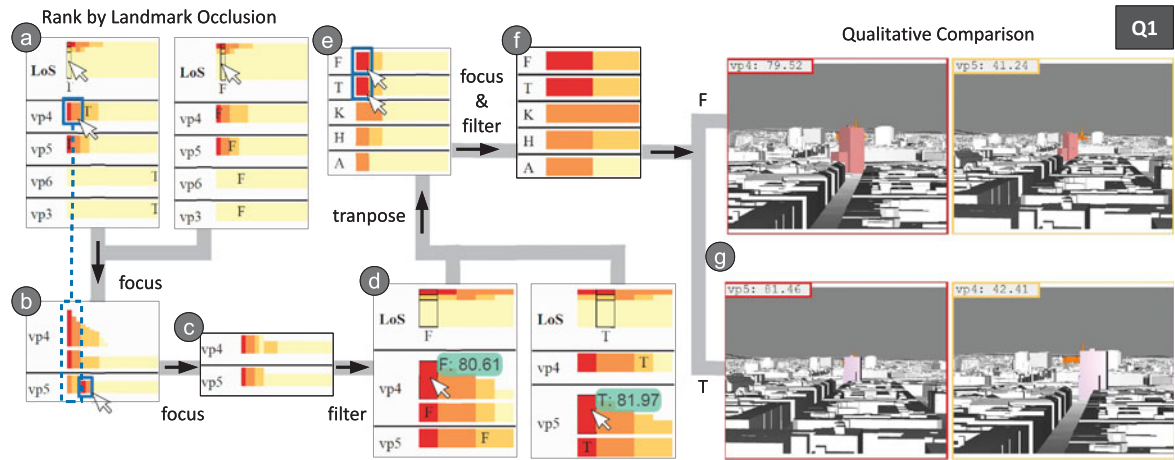


Fig. 7. Q1: Which candidates do cover a landmark and how strong is the occlusion? (a) Users rank by landmark occlusion and (b) focus on very high and high impact values. (c) All very high and high classes are part of the focus set and (d) filtering reduces the set of candidates to five. (e) To investigate top scoring candidates F and T in detail the TRV is transposed to candidate-major mode. (f) Users focus on viewpoints exhibiting very high impact values which are then assessed through (g) a qualitative comparison in the filmstrip.

building with a certain prominence and recognition value. To find the most prominent candidates along the railway users expand the 'Train' category in the TRV and rank the viewpoints by visibility. The 3D spatial view shows the distribution of affected viewpoints on the railroad (Fig. 8a). The sizes of the circles indicate that many viewpoints exhibit only a small coverage ratio, which deems these viewpoints as rather irrelevant for the question at hand. This is also reflected by the black circle in each viewpoint row as depicted in Fig. 8b. The aggregation shows multiple very high occurrences. The stacked bars however, reveal that these only occur in viewpoints with small coverage (*vp43*, *vp45*). Users consider viewpoints of large and medium coverage only and filter the TRV accordingly. Then they apply a series of focus, filter, and transpose interactions to reduce the set of viewpoints and candidates as shown in Fig. 8c. This is discussed in detail in Section 7.1.2 and Fig. 6. The interaction sequence begins with the reduced viewpoint set depicted in Fig. 6a. The aggregation view shown in Fig. 8d indicates that candidate *T* is most prominent as seen from the train tracks. However, peek-brushing the aggregation bars reveals vastly different distributions of the candidates *T* and *L*. Candidate *T* only has a medium score in the large coverage viewpoint *vp50*, while candidate *L* scores much higher in *vp50* and relatively high in the medium coverage viewpoints. Which candidate actually is considered to be more prominent is subject to discussion supported by a qualitative comparison in the filmstrip.

8.3 Which Candidates Have the Highest Impact on Sky and Openness in the Vicinity of the Project Area? (Q3)

As in the previous section, only viewpoints with a large or medium coverage value are considered. First, users sort the set of the 24 remaining viewpoints by openness occlusion, which reveals that for *vp63* all candidates have a very high openness score. Since this viewpoint is not very decisive, users select very high classes in the other viewpoints (Figs. 9a and 9b). Then they sort the viewpoints by sky occlusion, and select candidates with high sky occlusion values (Figs. 9c and 9d), and filter to the selected candidate subset

(Fig. 9e). Transposing the TRV depicts the remaining six candidates and allows users to select viewpoints which exhibit very high and high occurrences of openness occlusion and sky occlusion, respectively (Figs. 9f and 9g). After filtering to the selected set (Fig. 9h) users explore the highest scoring candidates through sorting by the respective VIM. As shown in Fig. 9i candidate *O* has the highest openness occlusion while candidate *T* causes the highest sky occlusion. If hovering over the candidate row the candidate building is highlighted in the spatial view. While further hovering over individual bars, the respective viewpoint glyphs are highlighted which allows users to assess the spatial distribution of impacted viewpoints.

8.4 User Feedback

During the design phase we collected feedback regarding prototype iterations of Vis-A-Ware with a gremium of ten participants from the departments of 'Urban Surveying' and 'District Planning and Area Usage' of Vienna. Additionally we discussed design decisions and VIMs with an urban planning expert. For the final evaluation we interviewed six domain experts from three different fields concerned with 3D visibility analysis: urban surveying (1), urban planning (2), and architecture and urban design (3). Each field was represented by two experts. Experts from 1 and 2 typically collaborate to create 3D visibility analysis products, while group 3 participates in the actual decision-making. In general the feedback from these sessions was very positive. Following a pre-defined protocol each evaluation started with an overview of the system to reintroduce the individual components and their interplay, followed by a recapitulation of the VIM computations. After an average period of twenty minutes for familiarizing themselves by actively using ranking, focus, filter, and transpose the experts found the interactions comprehensible and intuitive. Given the possibility for questions and support they could exercise through the three use cases presented in Section 8.

Users from 1 and 2 could immediately see that an interactive tool like Vis-A-Ware would improve their workflow by facilitating the evaluation of a large number of viewpoints

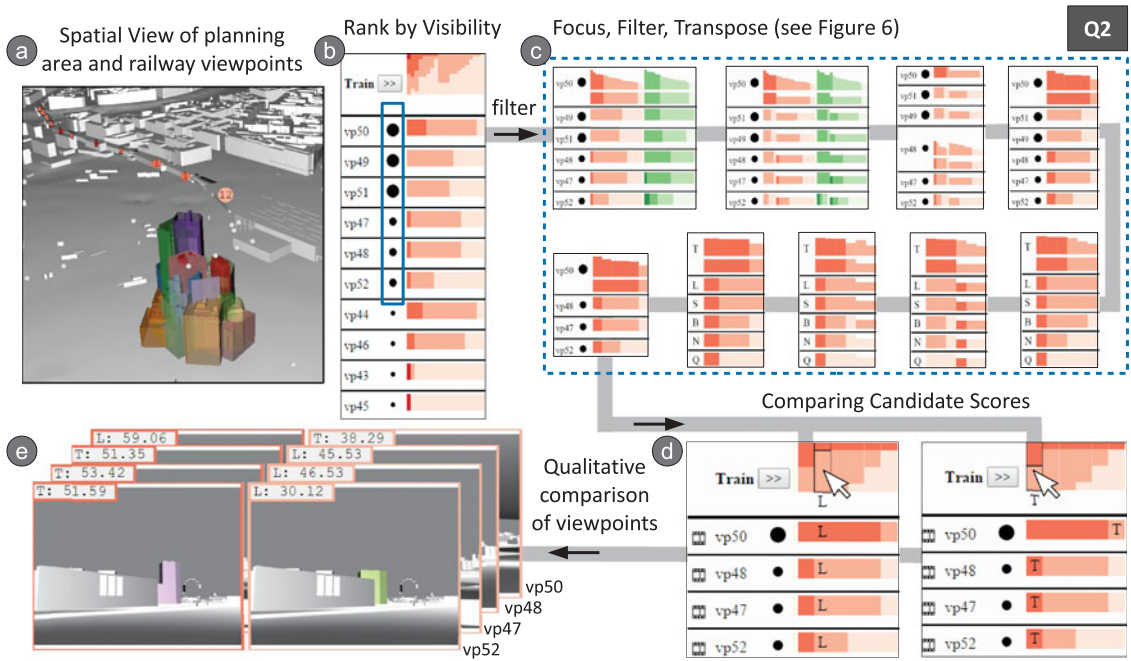


Fig. 8. Q2: Which candidates are most prominent as seen from the railway? (a) A spatial overview shows the distribution of the visibility impact as seen from the railway. (b) Viewpoints are sorted by candidate visibility. (c) Candidates and viewpoints are reduced through multiple focus, filter, and transpose interactions as illustrated in Fig. 6. (d) Peek-brushing of the highest scoring candidates reveals their scores within the distributions. (e) The remaining candidate-viewpoint combinations can be compared qualitatively in the filmstrip.

along streets. Further they stated that our approach for LoS evaluation and landmark occlusion is a very fast and intuitive alternative to time-consuming 2D visibility maps computed by GIS applications. They envisioned to use Vis-A-Ware as their primary tool for collecting and quantifying

visibility data. They welcomed the integration of an objective measure of visibility (i.e., VIMs) with the qualitative analysis provided by the filmstrip and the 3D spatial view.

The direct visual linking between spatial distribution and VIM values was appreciated as well, because it allows users

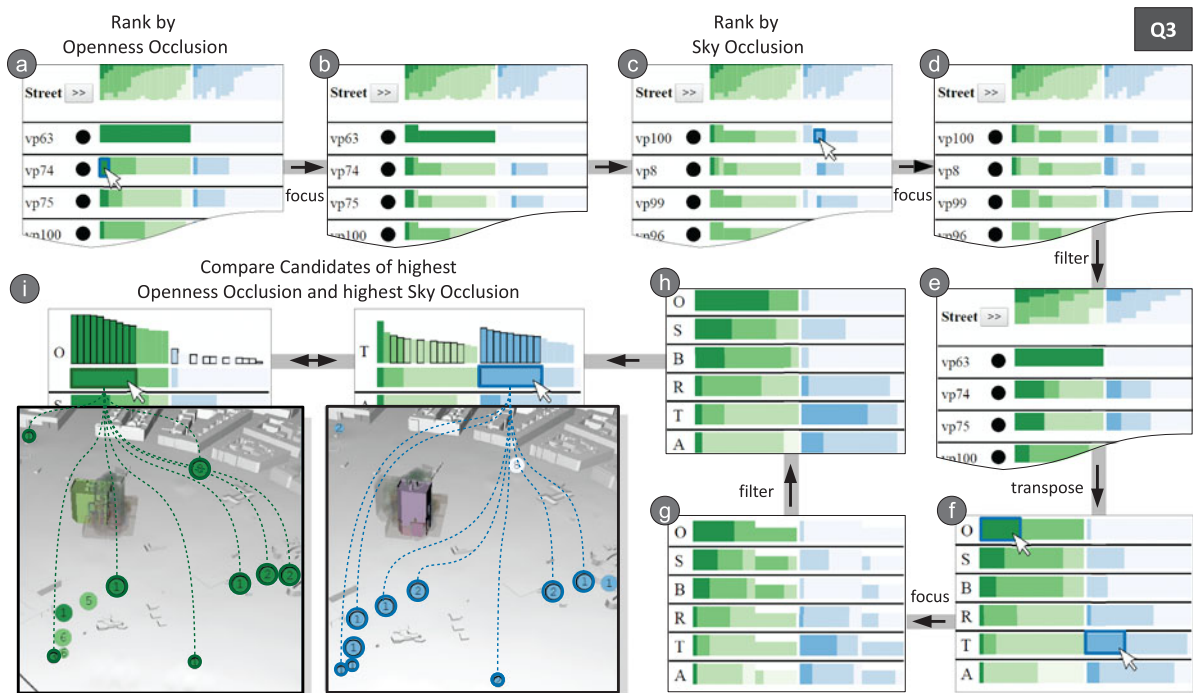


Fig. 9. Q3: Which candidates have the highest impact on sky and openness in the vicinity of the project area? (a) Users rank viewpoints by the openness metric and focus on (i.e., select) very high values of openness occlusion. (b) The focus set now contains all very high openness values ignoring vp63. (c) Then users rank by sky occlusion and select high values. (d) The focus set contains all high sky occlusion values. (e) Then users filter candidates which are not in focus. (f) Transposing the view lets the users investigate the remaining six candidates. (g) They again focus on viewpoints exhibiting very high openness occlusion and high sky occlusion and (h) filter to the focus set. (i) Sorting by either openness impact or sky impact yields the top ranked candidates O and T respectively. Hovering over candidate rows and viewpoints shows detail bar charts and results in the highlighting of buildings and viewpoint circles in the spatial view.

to judge which parts of the city are impacted on a granular level. Users from 1 and 2 pointed out, that Vis-A-Ware could efficiently evaluate whole streets, which has been a tedious task in the past.

When trying to comprehend the meaning of individual metrics, users of group 1 and 2 sometimes had difficulties to interpret the rather abstract VIM values for candidate visibility, openness occlusion, and sky occlusion. They stated that they would benefit from an attribute indicating the shape of a candidate. Two candidates, one tall, one wide, could essentially have the same sky occlusion value but both candidates would have a different perceived impact on the cityscape. Further, they questioned the relevance of the openness occlusion metric, since investigations about openness occlusion are typically not part of their analyses. They were very fond of the implementation of the landmark occlusion metric since it allowed them to quickly identify viewpoints from where the cathedral is occluded. They were able to judge the degree of occlusion quantitatively through the bar charts and verify it qualitatively through the images in the filmstrip.

Decision-makers (experts from group 3) are not the primary user group of the presented tool, since only a selected subset of viewpoints is presented to them for qualitative comparison. However, they could see the benefits of using the spatial view of Vis-A-Ware in jury discussions, where also project neighbors and political decision-makers are involved. Discussing a miniature model of the cityscape and candidates the decision-makers assess the visual impact from a bird's eye viewpoint. This issue is currently alleviated by placing a miniature camera into the haptic model. Vis-A-Ware could present pedestrian viewpoints interactively. Further the experts from group 3 were very interested in exploiting the interactivity of the tool. They suggested to perform and visualize evaluations along paths, such as signature streets or tourist walks, with different movement profiles (e.g., pedestrian, bicycle, or car) and playing back animations along these paths. Further they wanted to employ Vis-A-Ware to evaluate an upcoming high profile project regarding a new museum.

The user feedback tells us that Vis-A-Ware makes visibility analysis for experts from groups 1 and 2 more holistic, more objective, and less time-consuming. For experts from group 3 Vis-A-Ware presents opportunities to evaluate, analyze, and visualize dynamic movement paths.

9 IMPLEMENTATION

For the interactive rendering of the 3D urban scene we use an in-house real-time rendering engine [30] written in F# [31]. The TRV and the filmstrip are HTML5 pages displayed in a chrome browser, utilizing d3.js [32]. The viewpoint circles are also rendered to an HTML5 page, which is integrated as an overlay into the 3D view with the help of Chrome Embedded Framework (CEF) [33]. Both parts, the F# application and the HTML5 views, are communicating by exchanging JSON messages over a WebSocket communication layer. The tool as is, or individual parts of it, are not publicly available at this time.

We use a system comprising an Intel i7-3770 quad-core CPU running at 3.40 GHz, 16 GB of Ram, and a GeForce

GTX 680 graphics card. The 3D rendering runs smoothly at 50-70 frames per second, while rendering 500 k of triangles for buildings and 6,000 k faces for the terrain. We evaluated 20 candidate buildings against 106 viewpoints resulting in $2,332 = (20 + 2) * 106$ evaluations including the existing situation and the 'all candidates' images. For the VIM computations, we rendered 2,332 false-color images of reduced size (640×480 pixels) which took approximately 50 seconds. Taking 2,120 screenshots (1,280×960 pixels), one for each viewpoint-candidate pair, for a qualitative analysis took approximately 277 seconds. The smaller false-color images are processed in-memory, while the larger screenshots are saved to the hard disk, which is the most expensive step of the evaluation. With the given system and quality parameters we can process $7.1 = (2,332 / (277 + 50))$ candidate-viewpoint pairs per second.

10 DISCUSSION

At this point we summarize the key aspects of Vis-A-Ware and relate them to the design goals formulated in Section 1. We defined four metrics to quantify the visual impact of candidate buildings - landmark occlusion, candidate visibility, openness occlusion, and sky occlusion (G1). The transposable ranking view visualizes distributions of these metrics with respect to candidates and viewpoints. The distribution visualization provides a detail view on individual evaluation values (G3). The TRV provides interactions for ranking, focusing, filtering, and transposing of the data set (G3, G5, G6). Contents of a TRV row can at all times be loaded into the filmstrip which enables users to access image data for a qualitative analysis (G2, G6). Linked peek-selection connects entities in all views by hovering and highlighting (G2, G4). The 3D spatial view allows users to interactively explore the scene, which provides spatial context for candidates and viewpoints including their evaluation values.

10.1 Visual Scalability

The TRV in viewpoint-major mode provides a clear overview of viewpoints and scores of dozens of candidates through aggregation. The stacked bar chart representation is designed to efficiently use vertical space. Through categorization of viewpoints and filtering of viewpoints with low coverage, the number of viewpoints considered at once can be reduced significantly. Alternating filter and transpose interactions enable users to break down the problem space into a small set of entities to be inspected in detail. The current implementation of the TRV supports four different metrics. However, it could be extended to an arbitrary number of metrics, by aggregating, resizing, or collapsing of columns as presented in Gratzl et al. [17]. The underlying data model already supports an arbitrary number of metrics per evaluation

10.2 Applicability and Generalization

The developed tool features several linked views for a quantitative and a qualitative analysis of multiple visual impact metrics of candidates with respect to viewpoints. This approach directly translates to many visibility-related decision problems commonly solved with GIS-tools. For instance, in military planning different path options can be

evaluated for their exposure with respect to enemy positions and vantage points.

We can abstract our approach from candidates, viewpoints, and visibility analysis to the more general terms of discrete variations, probes, and simulation. Applied to a disaster management use case, we could consider a flooding simulation, where different barricading plans exist as discrete variations and important buildings act as probes for damage values. Users could easily identify bad barricading plans and buildings prone to flooding.

The TRV, as the center piece of this design study, can be used for ranking alternatives in any multi-criteria decision problem, such as, building design parameters [7] or sites for urban development [21]. It could also help to explore a large number of public utility issues in the context of districts and responsible departments [19]. The TRV is designed to explore a two-dimensional matrix, where each cell contains a vector of arbitrary length. It could support biologists in studying gene expressions, where they typically have to explore multiple potentially large heatmaps.

10.3 Limitations and Future work

Expert feedback showed that Vis-A-Ware has clear benefits over traditional, purely qualitative workflows. However, based on feedback sessions and design discussions we could identify points of improvement and opportunities for new features as future work:

- Whereas experts could easily relate to landmark occlusion, candidate visibility, and sky occlusion, the meaning of the openness occlusion was deemed as rather unintuitive. We believe this lies in the volumetric nature of openness perception as described by Yang et al. [1]. Extending our evaluation approach by additionally comparing depth images could yield more meaningful results and could actually quantify the volume of the open space occluded by a candidate.
- The 3D visibility analysis is a crucial, but actually small part in the decision-making process. There are many non-visual parameters, such as expected revenue or number of apartments and offices, which factor into a final decision. Extending the columns of the TRV, as discussed in Section 10.1, by non-visual parameters or scores from traditional automatic MCDA algorithms could make Vis-A-Ware a holistic tool for decision-making in urban planning.
- Candidate buildings potentially cast unwelcome shadows onto public squares or neighboring houses. While the TRV could be extended by a derived shadow VIM, the computation of that value and the qualitative comparison of cast shadows in the 3D spatial view over time are potentially challenging.
- Feedback from experts (in particular group 3 - architecture and urban design) indicated a need for evaluating visibility along paths with respect to different movement profiles. The current evaluation approach of Vis-A-Ware is suitable for computing VIMs along pre-defined paths. Designing a visualization for analyzing multiple visual impact metrics of 30 candidates over a spatio-temporal domain (movement profiles) poses an interesting challenge.

11 CONCLUSION

With Vis-A-Ware we present a design study to support analysts in quantifying and analyzing the visual impact of planned buildings in an urban environment. We developed linked views for a quantitative and a qualitative analysis of multiple output values of variations with respect to measurement probes. We illustrated the applicability of our approach based on a use case scenario involving complex visibility questions.

Qualitative feedback from experts of three different domains that are involved in the urban planning process confirmed that Vis-A-Ware enables a more holistic and efficient decision-making process. Experts from all three domains stated that they would be glad to incorporate Vis-A-Ware into their suite of tools.

ACKNOWLEDGMENTS

This work was supported in the scope of the FWF-funded project P24597-N23 (VISAR). The authors would like to thank Viennese ministry departments for their collaboration and their valuable feedback: MA 41 (Urban Surveillance), MA 21 (District Planning and Area Usage), and MA 19 (Architecture and Urban Design). Further they thank T. Höllt and T. Mühlbacher, and S. Zeddel for valuable comments.

REFERENCES

- [1] P. Yang, S. Y. Putra, and W. Li, "Viewsphere: A Gis-based 3d visibility analysis for urban design evaluation," *Environ. Planning B Planning Design*, vol. 34, no. 6, p. 971, 2007.
- [2] T. Akenine-Möller, E. Haines, and N. Hoffman, *Real-Time Rendering*. Boca Raton, FL, USA: CRC Press, 2011.
- [3] J. Bittner, M. Wimmer, H. Piringer, and W. Purgathofer, "Coherent hierarchical culling: Hardware occlusion queries made useful," *Comput. Graph. Forum*, vol. 23, no. 3, pp. 615–624, 2004.
- [4] M. Brunnhuber, H. Schrom-Feiertag, C. Luksch, T. Matyus, and G. Hesina, "Bridging the gap between visual exploration and agent-based pedestrian simulation in a virtual environment," in *Proc. 18th ACM Symp. Virtual Reality Softw. Technol.*, 2012, pp. 9–16.
- [5] ESRI. (2015). Arcgis [Online]. Available: <http://www.esri.com/software/arcgis>
- [6] Geoweb3d. (2015). Geoweb3d [Online]. Available: <http://www.geoweb3d.com/>
- [7] H. Doraiswamy, N. Ferreira, M. Lage, H. Vo, L. Wilson, H. Werner, M. Park, and C. Silva, "Topology-based catalogue exploration framework for identifying view-enhanced tower designs," *ACM Trans. Graph.*, vol. 34, no. 6, p. 230, 2015.
- [8] W. Berger and H. Piringer, "Interactive visual analysis of multiobjective optimizations," in *Proc. IEEE Symp. Vis. Anal. Sci. Technol.*, 2010, pp. 215–216.
- [9] S. Tarkkanen, K. Miettinen, and J. Hakanen, "Interactive poster: Interactive multiobjective optimization-A new application area for visual analytics," in *Proc. IEEE Symp. Vis. Anal. Sci. Technol.*, 2009, pp. 237–238.
- [10] H. Ribicic, J. Waser, R. Fuchs, G. Blöschl, and E. Gröller, "Visual analysis and steering of flooding simulations," *IEEE Trans. Vis. Comput. Graphics*, vol. 19, no. 6, pp. 1062–1075, Jun. 2013.
- [11] J. Waser, R. Fuchs, H. Ribicic, B. Schindler, G. Blöschl, and E. Gröller, "World lines," *IEEE Trans. Vis. Comput. Graphics*, vol. 16, no. 6, pp. 1458–1467, Nov./Dec. 2010.
- [12] M. Sedlmair, C. Heinzl, S. Bruckner, H. Piringer, and T. Möller, "Visual parameter space analysis: A conceptual framework," *IEEE Trans. Vis. Comput. Graphics*, vol. 20, no. 12, pp. 2161–2170, Dec. 2014.
- [13] S. Jafari and N. Zaredar, "Land suitability analysis using multi attribute decision making approach," *Int. J. Environ. Sci. Develop.*, vol. 1, no. 5, pp. 441–445, 2010.

- [14] N. Andrienko and G. Andrienko, "Informed spatial decisions through coordinated views," *Inf. Vis.*, vol. 2, no. 4, pp. 270–285, 2003.
- [15] S. Bruckner and T. Möller, "Result-driven exploration of simulation parameter spaces for visual effects design," *IEEE Trans. Vis. Comput. Graphics*, vol. 16, no. 6, pp. 1468–1476, Nov./Dec. 2010.
- [16] J. Sorger, T. Ortner, C. Luksch, M. Schwarzler, E. Groller, and H. Piringer, "Litevis: Integrated visualization for simulation-based decision support in lighting design," *IEEE Trans. Vis. Comput. Graphics*, vol. 22, no. 1, pp. 290–299, Jan. 2016.
- [17] S. Gratzl, A. Lex, N. Gehlenborg, H. Pfister, and M. Streit, "Lineup: Visual analysis of multi-attribute rankings," *IEEE Trans. Vis. Comput. Graphics*, vol. 19, no. 12, pp. 2277–2286, Dec. 2013.
- [18] G. Andrienko, N. Andrienko, S. Bremm, T. Schreck, T. Von Landesberger, P. Bak, and D. Keim, "Space-in-time and time-in-space self-organizing maps for exploring spatiotemporal patterns," *Comput. Graph. Forum*, vol. 29, no. 3, pp. 913–922, 2010.
- [19] J. Zhang, E. Yanli, J. Ma, Y. Zhao, B. Xu, L. Sun, J. Chen, and X. Yuan, "Visual analysis of public utility service problems in a metropolis," *IEEE Trans. Vis. Comput. Graphics*, vol. 20, no. 12, pp. 1843–1852, Dec. 2014.
- [20] W. Zeng, C.-W. Fu, S. M. Arisona, A. Erath, and H. Qu, "Visualizing mobility of public transportation system," *IEEE Trans. Vis. Comput. Graphics*, vol. 20, no. 12, pp. 1833–1842, Dec. 2014.
- [21] N. Ferreira, M. Lage, H. Doraiswamy, H. Vo, L. Wilson, H. Werner, M. Park, and C. Silva, "Urbane: A 3D framework to support data driven decision making in urban development," in *Proc. IEEE Conf. Vis. Anal. Sci. Technol.*, 2015, pp. 97–104.
- [22] R. Fuchs and H. Hauser, "Visualization of multi-variate scientific data," *Comput. Graph. Forum*, vol. 28, no. 6, pp. 1670–1690, 2009.
- [23] D. L. Gresh, B. E. Rogowitz, R. L. Winslow, D. F. Scollan, and C. K. Yung, "WEAVE: A system for visually linking 3-D and statistical visualizations, applied to cardiac simulation and measurement data," in *Proc. Conf. Vis.*, 2000, pp. 489–492.
- [24] R. Jianu, C. Demiralp, and D. H. Laidlaw, "Exploring 3D dti fiber tracts with linked 2d representations," *IEEE Trans. Vis. Comput. Graphics*, vol. 15, no. 6, pp. 1449–1456, Nov./Dec. 2009.
- [25] J. Sorger, K. Bühler, F. Schulze, T. Liu, and B. Dickson, "neuroMap—Interactive graph visualization of the fruit Fly's neural circuit," in *Proc. IEEE Symp. Biol. Data Vis.*, 2013, pp. 73–80.
- [26] R. Chang, G. Wessel, R. Kosara, E. Sauda, and W. Ribarsky, "Legible cities: Focus-dependent multi-resolution visualization of urban relationships," *IEEE Trans. Vis. Comput. Graphics*, vol. 13, no. 6, pp. 1169–1175, Nov./Dec. 2007.
- [27] T. Butkiewicz, W. Dou, Z. Wartell, W. Ribarsky, and R. Chang, "Multi-focused geospatial analysis using probes," *IEEE Trans. Vis. Comput. Graphics*, vol. 14, no. 6, pp. 1165–1172, Nov./Dec. 2008.
- [28] W. Berger and H. Piringer, "Peek brush: A high-speed lightweight ad-hoc selection for multiple coordinated views," in *Proc. 14th Int. Conf. Inf. Vis.*, 2010, pp. 140–145.
- [29] C. Brewer and M. Harrower. Colorbrewer 2.0 [Online]. Available: <http://www.ColorBrewer.org/>
- [30] VRVis. (2015). Aardvark. [Online]. Available: <http://www.vrvis.at/projects/aardvark>
- [31] (2015). Microsoft-Research. F# [Online]. Available: <http://fsharp.org/>
- [32] M. Bostock, V. Ogievetsky, and J. Heer, "D³ data-driven documents," *IEEE Trans. Vis. Comput. Graphics*, vol. 17, no. 12, pp. 2301–2309, Dec. 2011.
- [33] M. Greenblatt. (2015). Cef [Online]. Available: <https://bitbucket.org/chromiumembedded/cef>



Thomas Ortner received the Graduate degree in computer graphics programming from the Faculty of Science and Engineering, University of Hull, United Kingdom, in 2008. After working for several years as a programmer, he started working toward the PhD degree at the VRVis Research Center for Virtual Reality and Visualization. His current research topics involve the integration of 3D real-time rendering and abstract visualization techniques.



Johannes Sorger received the Graduate degree in visual computing from the Faculty of Informatics, TU Wien in 2013. He is currently working toward the PhD degree at the VRVis Research Center for virtual reality and visualization. His current research interests include the integration of spatial and nonspatial data visualization, and parameter-space exploration in dynamic simulations.



Harald Steinlechner is a researcher at the VRVis Research Center for virtual reality and visualization and PhD student at the TU Wien. His research interests include algorithmics, computer graphics, and the visualization of massive, highly dynamic real-time data. He is currently working on techniques for speeding up the visualization of dynamic data by utilizing incremental evaluation.



Gerd Hesina received the master's and PhD degrees in computer science from TU Wien. He has experience in software development in various programming languages for 23 years, experience in 3D visualization projects for 13 years, and is a senior researcher and project manager at the VRVis Research Center since 2002. He is an author and a coauthor of several internationally refereed scientific papers. In addition to his work at VRVis, he is also lecturing at the University of Applied Sciences Technikum Wien.



Harald Piringer received the master's and PhD degrees from TU Wien. He is the head in the Visual Analysis Group, VRVis Research Center in Vienna, Austria. His research interests include visual analytics for simulation and statistical modeling with a focus on the integration in real world settings. He authored and coauthored more than 20 internationally refereed scientific publications, among them two best papers.



Eduard Gröller is a professor at the TU Wien and an adjunct professor of computer science at the University of Bergen, Norway. His research interests include computer graphics, visualization, and visual computing. He coauthored more than 240 scientific publications and acted as a cochair, IPC member, and reviewer for numerous conferences and journals in the field. He became a fellow of the Eurographics association in 2009. He received the Eurographics 2015 Outstanding Technical Contributions Award.

▷ For more information on this or any other computing topic, please visit our Digital Library at www.computer.org/publications/dlib.